HEFAT2008
5th International Conference on Heat Transfer, Fluid Mechanics, and Thermodynamics
1-4 July 2008, Sun City, South Africa
Paper Number: GA1

REVERSE ROTATION OPERATION OF A MULTI-STAGE AXIAL FLOW COMPRESSOR

A. Gill*, T. W. von Backström and T. M. Harms
Department of Mechanical and Mechatronic Engineering
University of Stellenbosch
South Africa

Abstract

An experimental investigation of the third quadrant (reverse rotation) performance, operation and the internal flow structures of a three stage subsonic axial flow compressor is described. The compressor used for this investigation has three repeating stages, and a design speed of 3000 rpm, a design mass flow rate of 2.7 kg/s and a blade tip relative Mach number of 0.2 at design point. The non-dimensional third quadrant pressure rise and torque characteristics for this machine have previously been determined. The steady-state inter-blade row flow-field was experimentally obtained by means of a five-hole cobra-type pneumatic probe and time-dependent phenomena were resolved by means of a 50 μ diameter cylindrical constant-temperature hot-film sensor. The observed flow structures are compared with those observed in a single stage axial fan rotating in the reverse direction as described in literature. Flow within rotor blade passages is dominated by large areas of separated flow on the pressure surface of the blades. A large axial velocity gradient is observed in the radial direction, with velocities highest near the shroud. Third quadrant operation appears to be similar to stalled first quadrant operation. Separation was found to be less severe on the final stage rotor row, as this blade row functions as the inlet rotor row in this mode of operation, thus flow angles are less unsuited to blade metal angles. These results yield insight into the causes of the low maximum pressure rise and efficiency obtained for this operational mode for this machine, as well as the apparent lack of a stall point on the pressure characteristic obtained.

*Corresponding author: Department of Mechanical and Mechatronic Engineering, University of Stellenbosch, Private Bag X1 Matieland 7602, South Africa. Email at agill@sun.ac.za

INTRODUCTION

Axial flow compressors are commonly used in gas turbine engines, and are also used in process plants, and power generation schemes such as the proposed pebble bed modular reactor[1]. In disaster scenarios, the mean flow direction, direction of the pressure difference between the inlet and outlet of the machine, and direction of rotation of the rotor, may differ from that for which the machine was designed, and the operational point under such circumstances would thus appear in a quadrant other than the first quadrant on a compressor performance map relating pressure rise to flow rate.

This paper describes an experimental investigation of the inter-blade row flow fields occurring in one of these modes of operation, namely third quadrant operation, for the machine used in [2].

In order to explain third quadrant compressor operation, it is necessary to provide a brief description of four-quadrant compressor operation and the possible modes of operation therein. Gill et al.[2] identified six possible modes of operation and presented an investigation into the overall performance of the compressor for each mode. If the rotor remains stationary while air is forced through the compressor in the design and reverse directions, the resulting zero-speed total to static pressure characteristic forms an S-shaped curve composed of two parabolic curves which join smoothly at the origin and pass though the second and fourth quadrants. Two modes occur in each of these quadrants, as both positive and negative rotation are possible, and are separated by the zero-rotation S-curve. Only one mode is possible in each of the first and third quadrants, as the zero-speed curve does not pass through these quadrants; consequently negative rotation cannot occur in the first quadrant, nor positive rotation in the third. Static to static pressure rise characteristics were experimentally determined for all six modes. Gill et. al.[3] performed more detailed system measurements and improved

upon the accuracy of the previous study, as well as determining total to static pressure rise characteristics for the same machine.

Third quadrant operation occurs when the the the direction of rotation, mass flow and pressure rise all have negative signs. Power must be supplied via the rotor shaft in order to turn the rotor. Gill et al.[2] shows that this mode of operation is compressor-like, comparable to first quadrant operation, but overall performance (pressure rise and efficiency) are low compared to first quadrant performance, due to the direction of curvature of the blades relative to the flow.

Cyrus has conducted research into the third quadrant (reverse rotation) performance of an axial fan[4]. It was found that high rotor blade incidence angles compared with first quadrant operation were necessary in order to operate in the compressor regime, and that a significant degradation of performance occurred, largely due to flow separation in blade rows.

Cyrus[4] described an investigation of the reverse performance of two different single-stage axial fans with inlet guide vanes and adjustable outlet guide vanes. The aim of that investigation was to determine whether the fans investigated could achieve a reverse volumetric flow rate greater than a certain percentage of the design point volumetric flow rate, as it was considered desirable to be able to use the fans in reverse in some emergency conditions in industrial applications. A model was developed for third quadrant cascade flow, and experimentally verified. As a high volumetric flow in the reverse direction was desired, the possibility of improving third quadrant performance by adjustment of the outlet guide vanes was investigated. In a multi-stage axial flow compressor, this measure would have less effect, as stator stagger angles in stages downstream of the final stage are not usually adjustable, thus the flow angles in all stages except the final one are badly mismatched.

Also worth mentioning is the experimental investigation into second quadrant operation of an axial flow compressor by Gamache and Greitzer[5]. This investigation was performed on a 3-stage, non-repeating axial flow compressor at mean radius rotor blade Reynolds numbers varying between 1.0×10^5 and 2.0×10^5. These researchers determined that a discontinuity occurred where the second quadrant characteristic approached zero mass-flow rate, and that operation in this mode was characterised by strongly three-dimensional, unsteady flow. Although this investigation occurred in the second quadrant, that is for rotation in the design direction, flow conditions in this mode of operation are similar in that flow occurs in the reverse direction, and the blade metal angles are badly mismatched, resulting in heavily separated flow over the blades and highly unsteady flow phenomena, similar to an extreme case of first quadrant stalled operation. The time dependent hot-film velocity measurement set-up and scheme used in this investigation was based on the second quadrant hot wire investigations of these researchers.

EXPERIMENTAL FACILITY

Compressor

A three-stage axial flow compressor manufactured by the Royston Fan Co. Ltd. was used in the experimental investigation. The machine operates at a design speed of 3000 rpm, with a design mass flow rate of 2.7 kg/s, and a nominal total-to-total pressure ratio of 1.022. The entire operating range of the machine occurs within the subsonic incompressible regime, the first stage rotor having a relative blade-tip Mach-number of 0.2 when operating at design point. The relative rotor blade tip Reynolds number at design point is 1.5×10^5, although tests were conducted at a reduced speed, due to power limitations, leading to lower Reynolds numbers of the order of 1.25×10^5. The compressor has 43 rotor blades and 41 stator blades per stage. All stages are repeating and identical. It is fitted with NACA-65 blades on circular arc camber lines with the outflow from the stator blade rows in the axial direction. The reaction ratio of the compressor is approximately 0.82 at design point. The compressor has constant hub and casing diameters of 300 mm and 420 mm. The nominal blade length is 60 mm and the blade chords are 30 mm, with a maximum blade thickness 10 % of that value. The parameters defining the blades are given in Table 1. Spacing between rotor and stator rows in each stage is 22 mm at the mean radius, which is identical to the inter-stage spacing. Ports of 11 mm diameter allow the insertion of flow measurement probes or other instruments into the inter-blade row spaces, as well as before the first blade row, and after the last. There are no inlet or exit guide vanes.

The drive system consists of a direct current motor with a thryristor control system. The motor cooling fan exhausts air through an attached duct fitted with an axially aligned honey comb grid to ensure that the cooling air is swirl-free and does not exert a torque on the motor. The flow at the compressor exit is exhausted to a Venturi meter. An adjustable disk throttle is fitted to a threaded spindle mounted on the venturi outlet by means of a three legged spider. A schematic illustration of the experimental setup is shown in figure 1.

Blade section radial position (mm)	Blade profile stagger angle (degrees)	Blade profile camber angle (degrees)	Blade row solidity
ROTOR			
150.0	38.00	31.04	1.3051
165.0	45.00	23.48	1.1864
180.0	49.40	17.93	1.0876
195.0	53.00	13.85	1.0039
210.0	56.10	10.90	0.9322
STATOR			
150.0	20.38	46.28	1.3687
165.0	18.18	43.39	1.2443
180.0	16.61	41.05	1.1406
195.0	14.90	40.57	1.0529
210.0	14.32	40.00	0.9777

Table 1: Blade profile data for the Rofanco compressor

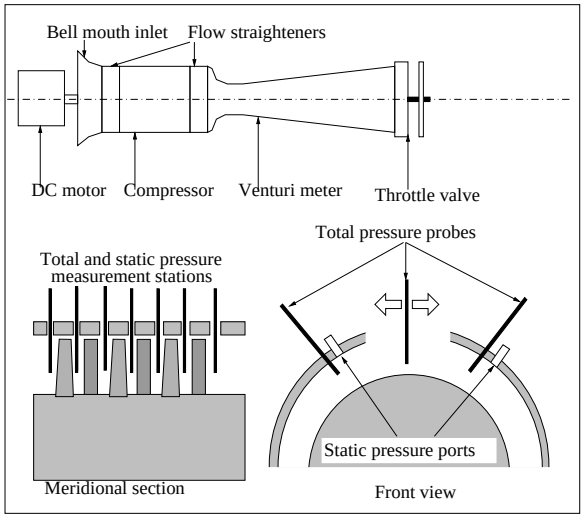

Figure 1: A schematic of the compressor test set-up

Instrumentation and Accuracy

Static pressure data was obtained from three tappings at circumferential positions 90^o apart at the compressor inlet, immediately upstream of the first rotor row, and at the outlet, immediately downstream of the last stator row. These were used to determine the static pressure rise across the compressor.

A five hole cobra-type pneumatic probe was used in all steady state radial and area traverses across the compressor annulus. The probe head is approximately 2 mm wide and 5 mm long. Errors in stagnation and static pressures as determined by the probe the probe are less than 4 Pa, while maximum errors in flow angles as determined by the probe do not exceed 1^o. However, in the presence of a large velocity gradient, such as is found in the boundary layer near the compressor casing, the probe yields artificially large flow angles due to finite probe head size, and the variation in stagnation pressure in the flow between the ports of the probe. This was likely exacerbated by the 11 mm ports through which the probe was inserted, which further disturbed the flow and boundary layer structure. The error thus introduced manifests itself as a sharp increase in the radial flow component at distances less than 10 mm from the compressor casing, an increase of approximately 10^o in the flow angle from the axis in the radial direction. This phenomenon was observed for both conventional operation near design-point (forward flow) and reverse-flow, reverse rotation (third quadrant) operation downstream of both rotor and stator rows. The boundary layer on the rotating hub is smaller and has a flatter velocity profile, therefore it introduces a smaller inaccuracy into probe measurements. For steady state investigations the sampling rate was 1000 samples per second per channel.

Pressures from the probe and tappings were recorded by means of seven AutoTran model 860 differential pressure transducers having a range of 2500 Pa.The rated error of these pressure transducers is 1% of the full scale output. However, statistical analysis of the transducer output demonstrated that the measurement error for all transducers was approximately 1.5 Pa, less than 0.001% of full scale output.

A 45^o inclined cylindrical hot film sensor of 20 μ diameter was used to for time-dependent inter-blade row flow measurements.The sensor was used in conjunction with an IFA 100 constant temperature thermal anemometer manufactured by TSI. The bridge amplifier in the anemometer unit has a noise rating of 2.5 nV/$sqrtHz$, and an input drift of0.35 ηV/^{o}C. Hot film data were recorded at 20000 samples per second, approximately 10 times the blade passing frequency for the rotor. 5000 samples were recorded, representing a period of approximately 10 complete rotor revolutions.

A vaned turbine type anemometer with a diameter approximately equal to the internal diameter of the Venturi-meter throat was used for volumetric flow measurements. This instrument was found to provide better accuracy at low mass flow rates and unsteady flow conditions such as stall.

All data were recorded by means of a National Instruments NI-USB6218 16-bit data acquisition unit.

RESULTS

The steady state and time-dependent flow field results will now be presented. To maintain consistency, the compressor inlet, outlet, blade rows and

stages refer to the position of each under first quadrant (conventional) operation. Thus, during 3rd quadrant operation, flow enters the compressor at the outlet (third stage stator) and exits at the inlet (first stage rotor).

Due to time constraints, the investigation was restricted to one operational condition, for an average rotational speed of 2440 RPM, an average mass flow rate of 0.96 kg/s and an average pressure difference between the compressor inlet and outlet of 580 Pa. This corresponds to a flow coefficient of -0.22 and a pressure rise coefficient of 0.34. This operating condition is attained when the throttle valve is opened to maximum, that is system resistance is at a minimum, thus it would have been necessary to make use of an auxiliary fan as described in [2] in order to attain a higher negative mass flow rate.

Steady-State Traverses

Figures 2, 3 and 4 show the spanwise axial and tangential velocity component profiles determined by means of the five-hole probe for the third, second and first stages respectively. Samples were taken in 2 mm intervals in the regions between 2 and 10 mm from the hub and the shroud, and at five mm intervals between these regions. Very little variation was observed in the flow angle from the rotational axis in the radial direction for any blade row, and the measured angles were less than 5^o, with the exception of the large angles observed very close to the casing, the probable causes of which have already been discussed in the preceding section. Radial flow in the inter-blade row regions can thus be neglected for this investigation. All velocity components are non-dimensionalised in terms of the rotor blade tip velocity.

The spanwise axial velocity component distributions downstream of each rotor row show large, well-defined velocity gradients,with the maximum axial velocity occurring near the blade tip. These gradients are approximately equal for all rotor stages, as all stages have identical geometry. However, there is some variation in the profiles near the hub and casing, mainly due to the fact that, in the third stage, the flow from the stator upstream is not separated, unlike the downstream stages. The traverses conducted downstream of the stator blade rows are not expected to be representative of the circumferential average flow condition, due to the fact that the position of the blades and hence the wakes relative to the probe head were unknown. For this reason, an area traverse was conducted downstream of the first stage rotor.

Figure 5 represents the velocity distribution downstream of the first stage stator for a rectangular area corresponding approximately to a sin-

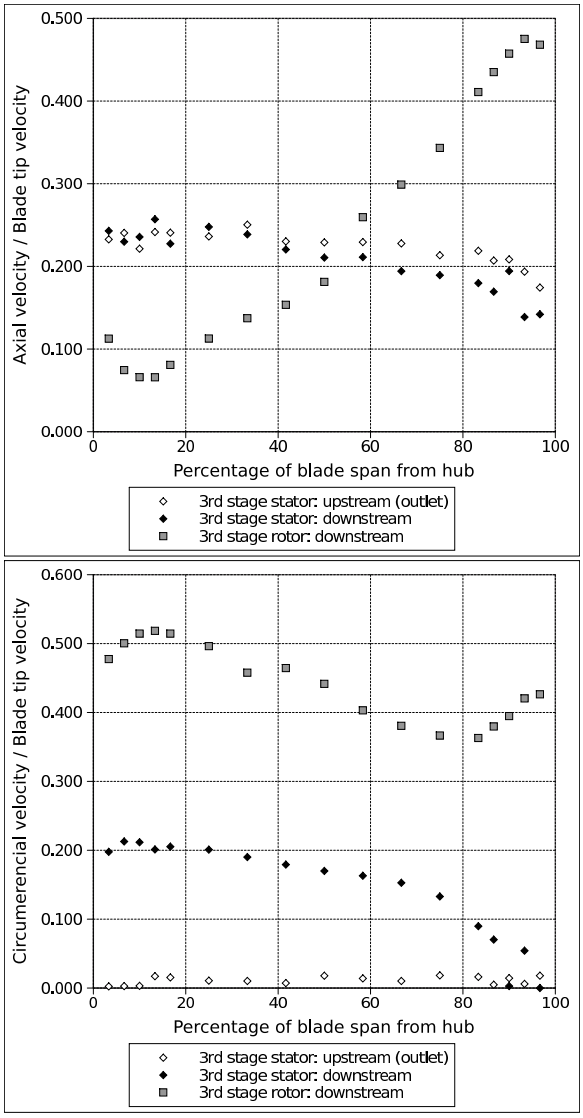

Figure 2: Spanwise variation of axial and circumferencial velocity components for the third stage

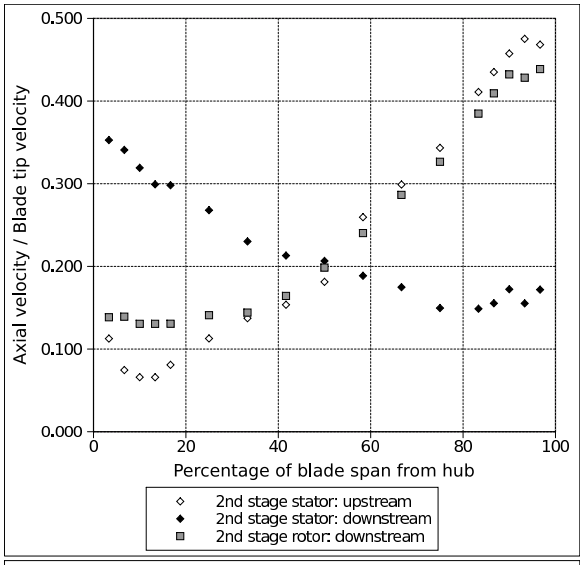

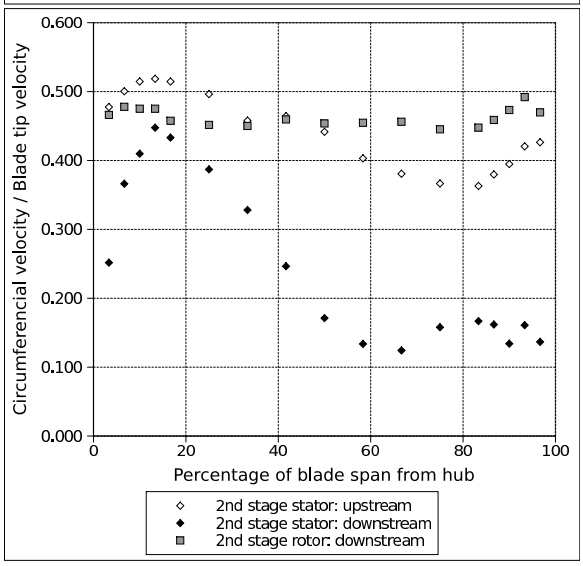

Figure 3: Spanwise variation of axial and circumferencial velocity components for the second stage

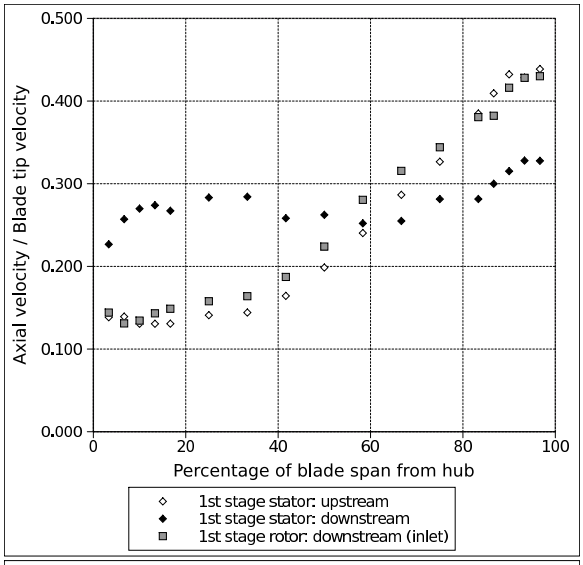

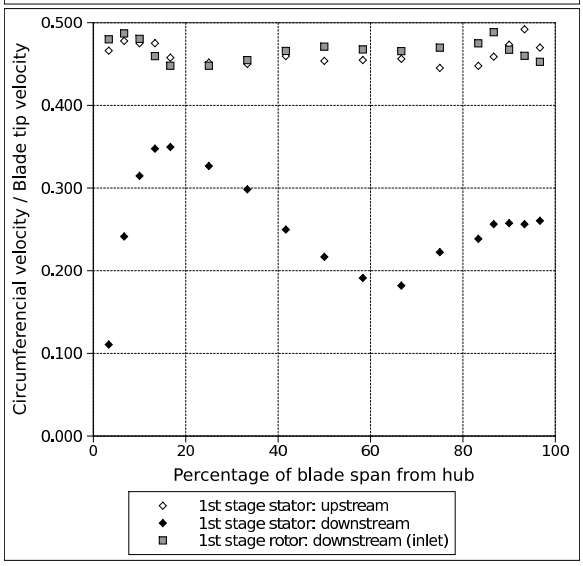

Figure 4: Spanwise variation of axial and circumferencial velocity components for the first stage

gle blade passage. The circumferential resolution was 5 mm. The radial sampling distribution was identical to that used for the radial steady state traverses. The first quadrant area traverse downstream of the same blade row is shown for comparison. It is evident that the third quadrant blade wake is considerably larger and more clearly defined than that of the first quadrant, suggesting that a large separated flow region exists on one or both of the surfaces of the blade. The separated region is largest and most pronounced near the shroud. Between wakes, two jets of higher velocity flow appear to exist: one near the hub and one near the shroud. Thus the velocity downstream of the stator row appears to exhibit an alternating wake-jet structure not unlike that observed by Gamache and Greitzer[5] in their second quadrant investigation. It would appear that the spanwise velocity distribution shown in figure 4 corresponds approximately to a transverse position between 25 and 30 mm from the datum in the third quadrant diagram of figure 5. Based upon the radial velocity components determined (figure 3, there is reason to believe that the area downstream of the second stage stator exhibits a similar flow structure, in particular a large wake caused by flow separation. Flow downstream of the final stage stator is relatively well ordered, however, as the flow entering this blade row, having no rotor row upstream to divert it from the axial direction, corresponds to the axial alignment of the blade trailing edges.

Following [4], the velocity triangles for the final stage (at which the flow enters) and all downstream stages can now be constructed, as shown in figure 6. The symbols C, W and U refer to the absolute and relative flow velocities and the rotor blade velocity respectively.

It is apparent that flow angles upstream of blade rows (at the trailing edges) will be more badly matched to the blade metal angles near the shroud than at the hub, due to the increase in the stagger angle with increasing radius in compressor blades. this is particularly apparent in the downstream stator area traverse, where the separated region of the wake is largest near the tip. This is also part of the cause for the large velocity gradient downstream of the rotors.

Time-Dependent Radial Traverses

As in [5], time dependent velocity measurements using a inclined cylindrical hot film sensor aligned with the flow were performed at five radii downstream of each rotor row. As a single sensor probe was used, the instantaneous velocity magnitude was determined, but it was not possible to determine the instantaneous magnitude of the three-dimensional velocity components. The time-

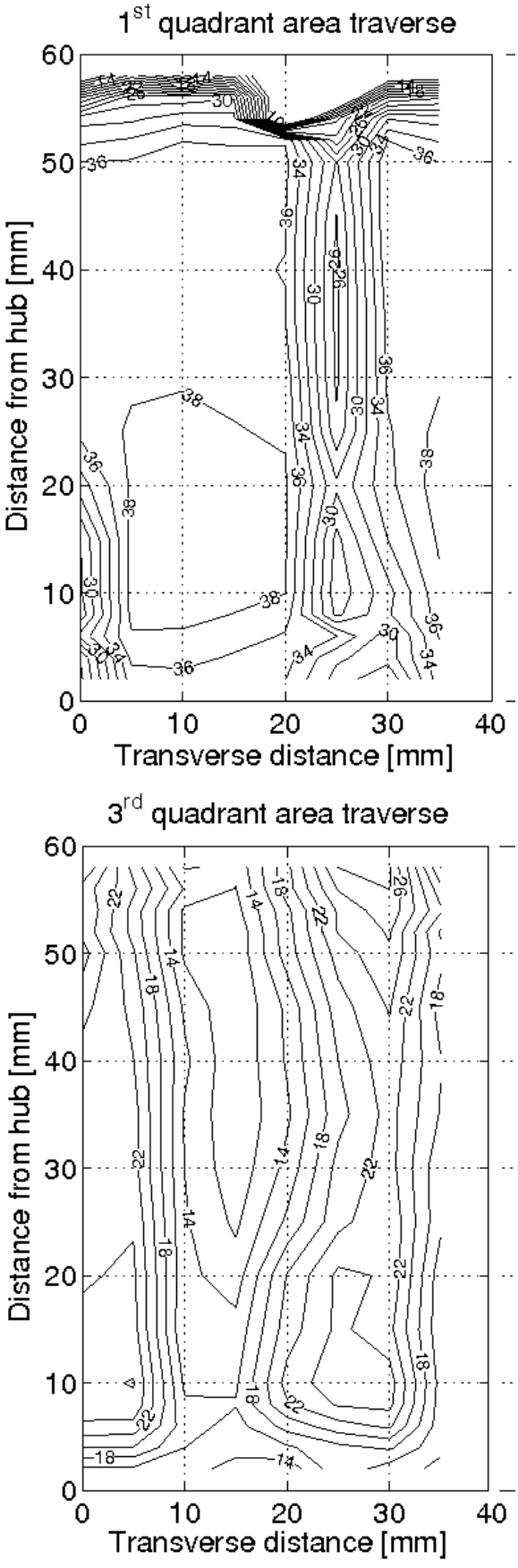

Figure 5: Velocity magnitude contour for plane downstream of first stage stator

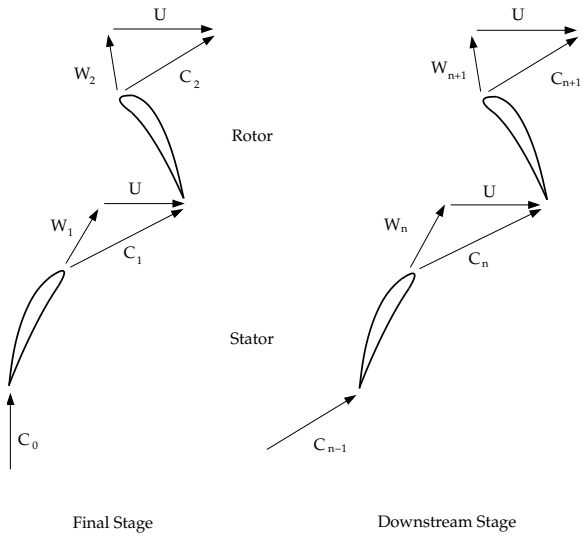

Figure 6: Velocity triangles for the final stage and upstream stages

averaged velocity magnitudes determined thus obtained agree very well with the steady-state velocity measurements, except for results downstream of the first stage rotor nearest the hub and shroud, as shown in figure 7. The time traces for the final stage rotor for one complete revolution are shown in figure 8.

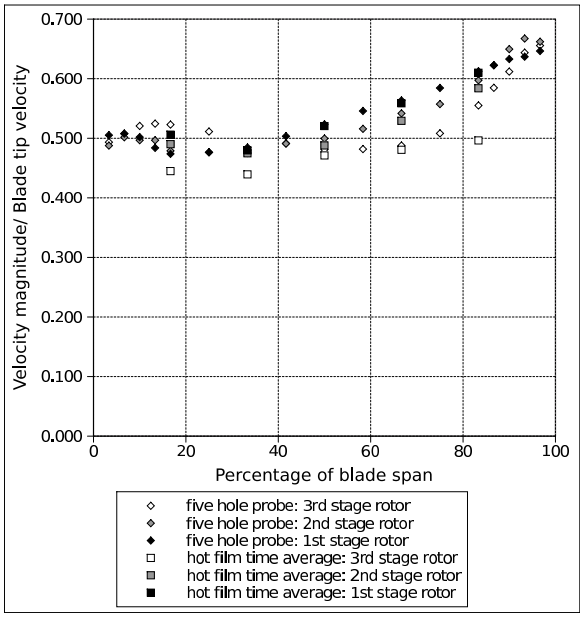

Figure 7: Time-averaged velocity profiles down stream of rotors measured with five hole and hot film probes

At all radii shown, the flow appears to be disordered, and the blade wakes are not easily identifiable. In order to identify cyclic phenomena in the time-traces, a Fourier analysis was performed on the data for each radius, as shown in Figure 9. In both cases the blade passing frequency is clearly indicated at approximately 1750 Hz.

For comparison, figures 10 and 11 show the velocity time trace and frequency spectrum obtained for the third stage rotor for near-design operation in the first quadrant. The compressor speed was approximately equal to that in third quadrant reverse operation, namely 2400 Hz, or 80% of design speed. It will be seen that the first quadrant time trace generally has a more cyclic, repeating, structure, than the corresponding third quadrant measurement, and the velocity variations recorded are of a considerably smaller, and more constant amplitude. Once again, the blade passing frequency is clearly indicated at approximately 1750 Hz. However, in this case, the second, third and fourth harmonics are also well defined, indicating that first quadrant rotor wakes are small and sharp, with large areas of approximately uniform velocity between them, as is the case with the stator wake examined in figure 5. In contrast, the harmonics of the blade passing frequency are not clearly evident at any radius during third quadrant operation, indicating that velocity variation in the circumferential direction is approximately sinusoidal downstream of the rotor in this mode of operation, and that the wakes are large and not well defined, occupying approximately half the blade passage. This, too, is similar to the wake structure observed downstream of the stator during third quadrant operation (Figure 5).

Another notable difference between the first and third quadrant frequency spectra is that for third quadrant operation, the magnitude of the blade passing frequency component relative to the other frequency components is smaller, suggesting that flow is highly turbulent. This is probably caused by the relatively disordered, separated flow occurring in this mode of operation.

It is thus apparent that flow downstream of rotor blade rows in third quadrant compressor operation is highly disordered and turbulent, with large variations in velocity relative to time. The frequency spectrum of the velocity as a function of time yields many comparatively large frequency components below the blade passing frequency. However, it was not possible to conclusively relate any of these frequency components with stall cells such as those examined by Day[6] at this time.

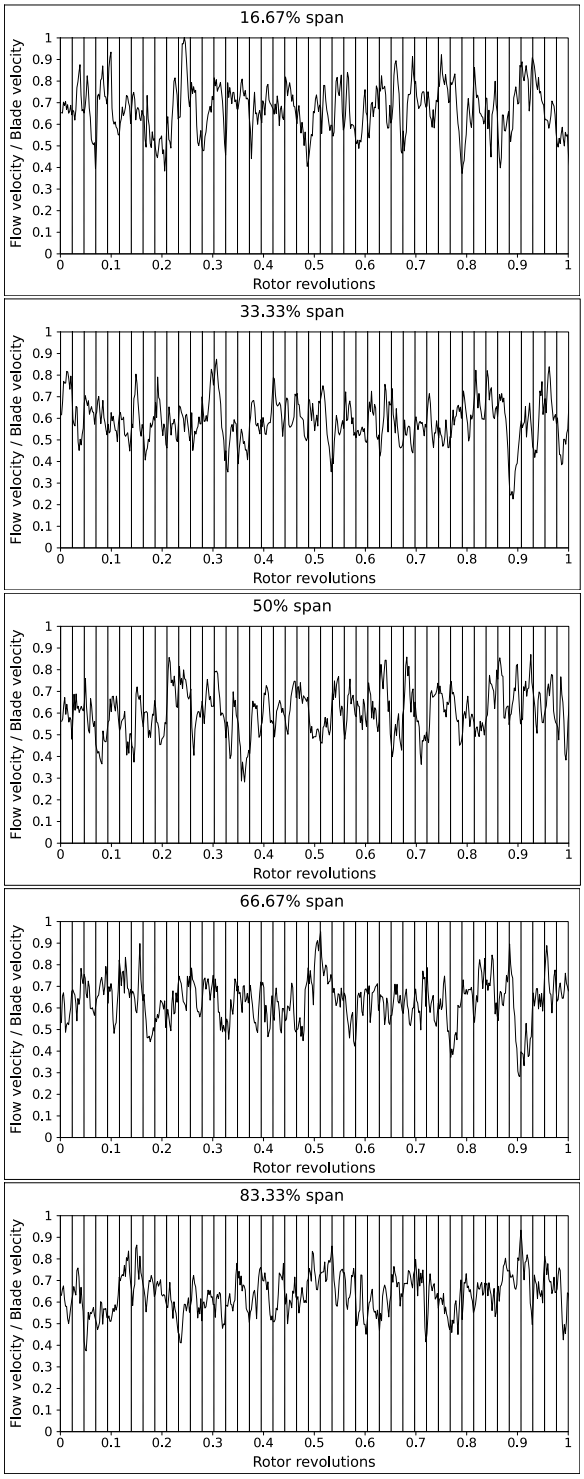

Figure 8: Hot film time traces at five radii downstream of 1st stage rotor during 3rd quadrant operation. *Dashed lines represent blade passing intervals.*

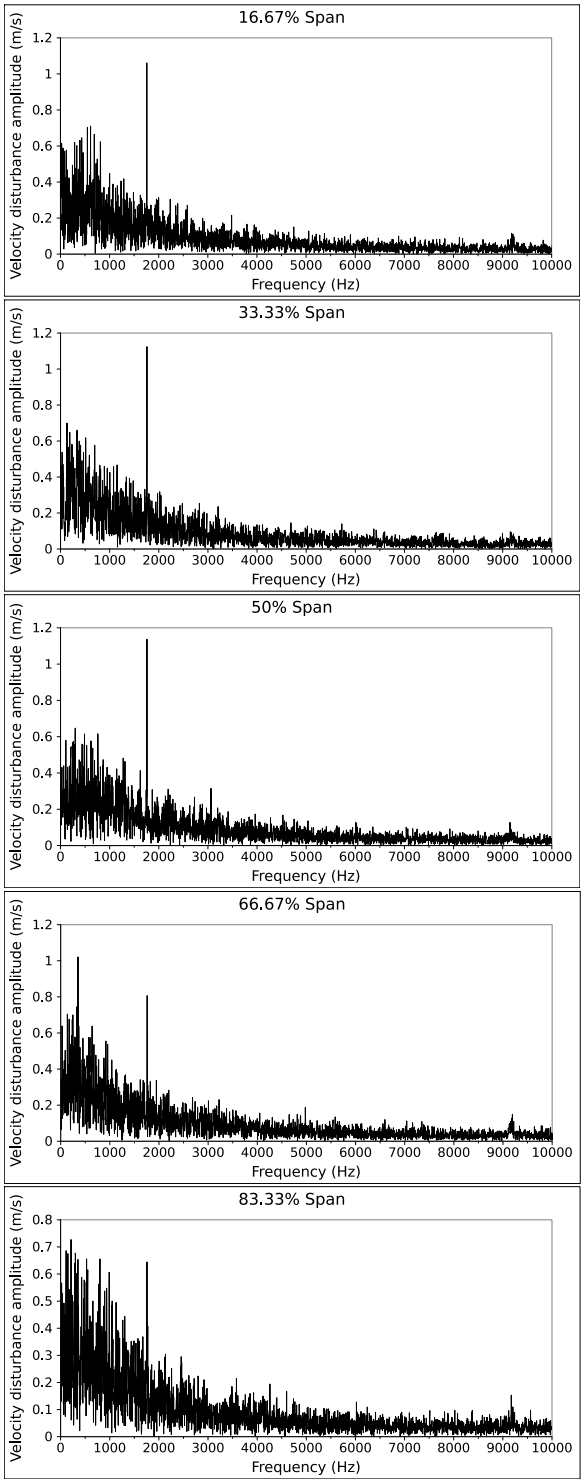

Figure 9: Hot film frequency spectra at five radii downstream of 1st stage rotor during 3rd quadrant operation

CONCLUSION AND SUMMARY

The steady-state and time dependent velocity distributions in the inter-blade row regions of a three stage axial flow compressor have been determined for one operational point in the third quadrant. The axial and circumferential velocity components downstream of the rotor exhibit a large gradient in the radial direction, having a minimum value near the hub and a maximum near the shroud. The area

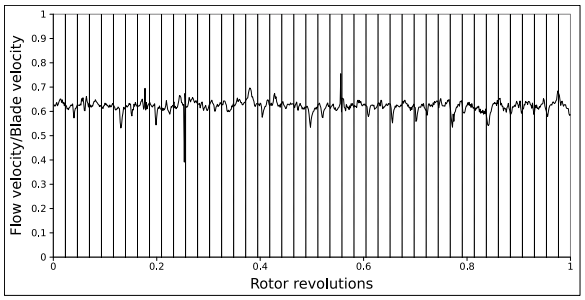

Figure 10: Hot film time trace at mid-span downstream of 1st stage rotor during 1st quadrant operation.*Dashed lines represent blade passing intervals*

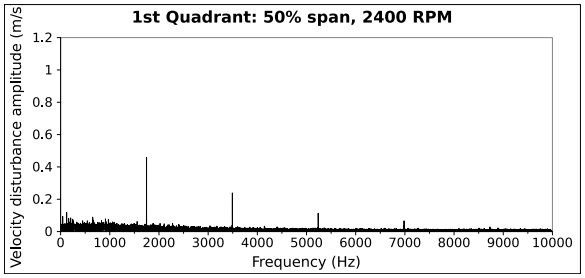

Figure 11: First quadrant (near design) hot film measurement frequency spectrum downstream of 1st stage rotor

downstream of the stator shows a wake-jet pattern similar to that of [5], with the wake larger and better defined than for first quadrant operation, particularly near the shroud. This suggests that flow in this region is severely separated from the blade.

The time-dependent velocity distribution downstream of the rotors shows large variation of velocity magnitude in time. The variation of velocity with time is larger and less well structured than that observed at the same rotational speed during first quadrant operation. Blade wakes are difficult to identify, though the blade passing frequency and its harmonics may be extracted by examination of the frequency spectrum of the velocity as a function of time. However, the frequency components lower than the blade passing frequency were larger in relation to that quantity than for first quadrant operation. However, there was no clear evidence of rotating stall cells in this region. This may be because flow is disordered around the entire annulus, due to the extreme misallignment of the blade trailing edges with the oncoming flow.

ACKNOWLEDGEMENTS

The authors wish to thank the NRF for funding this research.

References

[1] A. Koster, H.D. Matzner, and D.R. Nicholsi. Pbmr design for the future. *Journal of Nuclear Engineering and Design*, 222:231–240, 2003.

[2] A. Gill, T. W. von Backström, and T. M. Harms. Fundamentals of four quadrant axial flow compressor maps. *Proceedings of the IMechE part A: Journal of Power and Energy*, 221(A7):1001–1010, 2007.

[3] A. Gill, T. W. von Backström, and T. M. Harms. Four quadrant total to static characteristics of an axial flow compressor. *Proceedings of the Fifth International Conference on Heat Transfer, Fluid Mechanics, and Thermodynamics, HEFAT2007*, (GA1), 2007.

[4] Vaclav Cyrus. Axial fan at reverse flow. *Proceedings of ASME Turbo Expo 2004: Power for Land, Sea an Air*, pages 437–446, 14-17 June 2004.

[5] R. N. Gamache and E. M. Greitzer. Reverse flow in multistage axial compressors. *International Journal of Turbo and Jet Engines*, 6:461–473, 1990.

[6] I. J. Day. Stall inception in axial flow compressors. *ASME Journal of Turbomachinery*, 115:1–9, 1993.